Journal of the Optical Society of Korea, Vol. 4, No. 1, March 2000, pp. 1-6

Pupil plane wavefront sensing with a static pyramidal prism: Simulation and preliminary evaluation

Jun Ho Lee*

Earth Observation Payload Development Division Satellite Technology Research Center
KAIST, Taejon 305-701, KOREA
E-mail : jhl@satrec.kaist.ac.kr

A.P.Doel and D.D.Walker

Dept. of Physics and Astronomy University College London
**London University, U.K.*

(Received October 14, 1999)

Adaptive optics (AO) removes or compensates the distortion caused by a turbulent atmosphere or medium. A wavefront sensormeasures the distortion, on which the correction of AO is based. A new idea of pupil plane wavefront sensing, which consists of a relay lens and a pyramidal-shaped prism, was previously proposed. This paper reviews the idea of pupil wavefrontsensing and presents the results of simulation and preliminary evaluation of this approach. The simulation shows that pupilwavefront sensing provides full wavefront sensing when the intensity peak of PSF is located within half of the Airy radius from the apex of the sensor. Adding to this, the sensor is shown to have optimum sensor output with a finite bevel size of the pyramidal prism.

I. INTRODUCTION

Adaptive optics (AO) corrects the wavefront distortion caused by the Earth's atmosphere (or other turbulent medium) in realtime. [1] These distortions are basically spatially and temporally random. A keycomponent of an AO system is the wavefront sensor, the function of which is to measure thewavefront distortion. Current AO systems use a range of wavefront sensor designs employingdifferent sensing methodologies, the main ones being: the shearinginterferometer [2,3], the Shack-Hartmann wavefront sensor [4,5], and thecurvature wavefront sensor. [6,7] The first two sensors measure wavefront tilts(gradients) while the last one measures curvature directly.

Pugh [8] and Ragazzoni [9] independently proposed a new approach to wavefrontsensing called pupil plane wavefront sensing. It has a simple sensor configuration (Fig. 1)which is relatively free of mechanical alignment problems and avoids the fabrication ofexpensive custom components such as lenslet arrays. It comprises a pyramidal prism (or a pairof crossed biprisms) which act as star image splitters in the telescope image plane, splittingthe incident wave into four beams. The prism is followed by a relay lens which forms fourpupil images. These may be recorded by four separate area detectors, or projected onto fourquadrants of one detector. These pupil images exhibit intensity differences related to the phasegradient of the incident wavefront.

Ragazzoni [9] points out that pupil plane sensing with an oscillating pyramidalprism can change both gain and sampling easily in a simple and continuous manner, by changingthe amplitude of the oscillation and the focal length of the relay lens respectively. It has advantage over the conventional wavefront sensors for which it is hard tochange sampling. This is true especially for Shark Hartmann sensors where sampling modificationneeds a change of lenslet array, which is difficult in practice due to alignmentproblems.

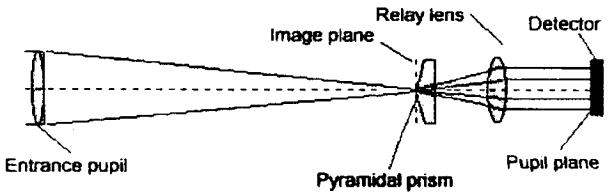

FIG. 1. Schematic diagram of the optical layout of the wavefront sensor [8].

Pugh [8] used a pair of static crossed biprisms, which are essentially identical to asingle pyramidal prism, whilst Ragazzoni [9] used an oscillating pyramidal prism. Theprimary advantage of the biprisms is ease of manufacture, since it is easier to polish a sharpedge than a point. Since Pugh uses static biprisms, Pugh's approach allows the simpleimplementation but not the change of the gain of the device against measured wavefrontdeformation.

This paper follows and extends Pugh's works and presents results from simulations of the sensor together with preliminary laboratory evaluation of a prototype sensor. However, the results of this paper provide a sound basis for theresearch of Ragazzoni's approach as well.

II. DESCRIPTION OF THE PUPIL PLANE WAVEFRONT SENSOR

The wavefront sensor layout is sketched in Figs. 1 and 2. In a true implementation, an achromat doublet is used as arelay lens.

The nominal focal plane of the telescope illuminating the wavefront sensor lies approximately on the vertex of the pyramidal prism. The light hitting the four faces of this prism is deflected in slightly different directions and, as seen from the relay lens, the exit pupil position of the telescope will appear slightly shifted in four different directions. Therefore four apparent exit pupils are conjugated by the relay lens onto four pupil images on the detector surface. The vertex angle of the pyramid is to be kept very low to give the four pupils enough relative displacement so they do not overlap (as in Fig. 2). [8,9] The amount of light that is collected by one pupil is given by the amount of light that hits the prism on the related face. Based on this, Ragazzoni [9] shows

$$\frac{\partial W}{\partial x} = C\frac{(a+b)-(c+d)}{a+b+c+d}$$

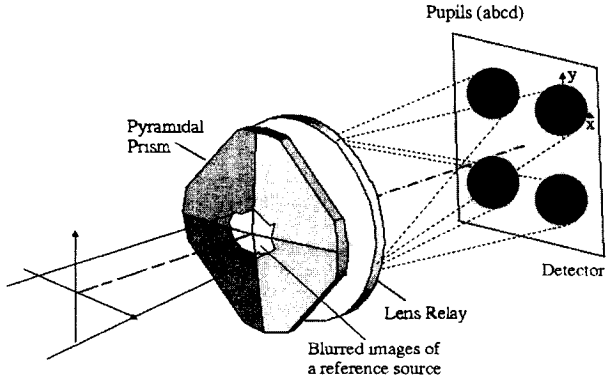

FIG. 2. 3D Schematic diagram of the optical layout of the wavefront sensor [9].

$$\frac{\partial W}{\partial y} = C\frac{(a+c)-(b+d)}{a+b+c+d} \quad (1)$$

where a, b, c, d represent the intensity distribution on the four pupil images (Fig. 2) andx, y are the normalised coordinates on the pupil plane ($x^2+y^2=1$ on the edges of the pupil, both in the realand in the reimaged ones). W is the wavefront and C is a constant. The equation indicates thatthe local tilts of the wavefront can be obtained by arithmatical manipulation of theintensities of the four pupil images.

III. SIMULATION

Wavefront sensors measure input wavefront distortions in terms of a set of coefficients of known function. Sensitivity and linearity of the coefficients to input wavefront distortions are important features of a sensor, particularly if it is to beused to close the loop in an adaptive optics system. In order to investigate the sensitivity and linearity of the pyramidal prism sensor against various Zernike distortions, the following simulations were performed.

The simulation begins with a generation of a distorted wavefront across a telescope aperture. The Fourier transform of this gives the point spread function (PSF) of the telescope. This is then dissected into four quadrants, each of which is further transformed to return to the pupil plane. This therefore gives the pupil image formed by that quadrant of the PSF.

The first 13 Zernike (Noll's definition [12]) terms were generated on 128 × 128grid, circularly masked, in the centre of a 256 × 256 array, in a commercial matrixcalculation program (MATLAB [10]). Based on a basic sampling theorem [11], thewidth of the square matrix (256 pixels) was set to be twice the size of the telescope diameter(128 pixels) to prevent overlapping of the sampling in the Fourier plane. The Fourier transformwas performed using a Fast Fourier Transform provided in the commercial program. Fig. 3 showsthe four quadratic simulated pupil images on the detector for the first 13 Zernike terms.

A set of sensor signals was then calculated, similar to a quad-cell, from the intensity distribution of the four subapertures using the following equations: (see Eq. (1))

$$t_x(i,j) = \frac{(I_a(i,j)+I_b(i,j))-(I_c(i,j)+I_d(i,j))}{(I_a(i,j)+I_b(i,j)+I_c(i,j)+I_d(i,j))} \quad (2)$$

$$t_y(i,j) = \frac{(I_a(i,j)+I_c(i,j))-(I_b(i,j)+I_d(i,j))}{(I_a(i,j)+I_b(i,j)+I_c(i,j)+I_d(i,j))} \quad (3)$$

where $I_n(i,j)$ is the intensity at position(i,j) of the n^{th} quadrant (Fig. 2) and$t_x(i,j)$ and $t_y(i,j)$ are respectively x and y component of the sensor signal at (i,j)in the aperture.

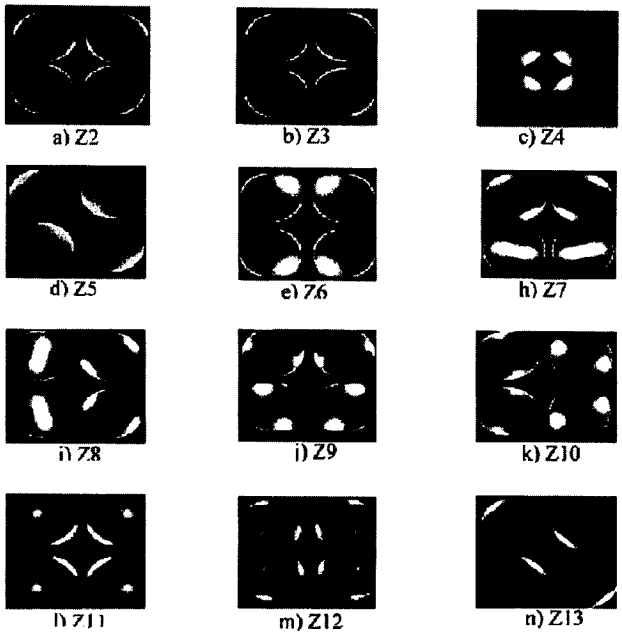

FIG. 3. Simulated pupil images on a single array detector for the first 13 Zernike terms

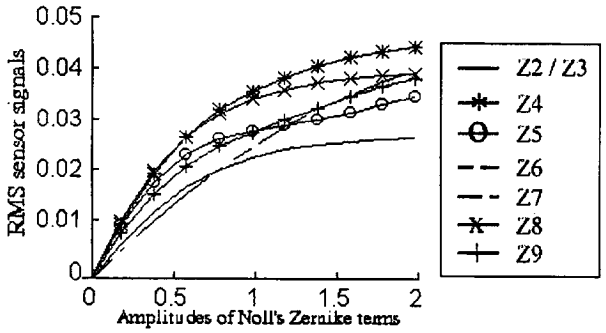

FIG. 4. Sensitivity (RMS sensor signals) for the first 8 Zernike terms of various amplitudes (unit radian)

III. A. Sensitivity

Fig. 4 plots RMS values S_{RMS} of the sensor signals $t_x(i,j)$ and $t_y(i,j)$ as definedby

$$S_{RMS} = \sqrt{\frac{\sum_i \sum_j (t_x(i,j)^2 + t_y(i,j)^2)}{\sum_i \sum_j 1}} \tag{4}$$

The value S_{RMS} represents how strong the RMS intensity of sensor signals is for a givenwavefront aberration so it might be a measure to show the sensitivity of the sensor to thegiven wavefront aberration. Fig. 4 shows that the sensitivity of the sensor to the lowerZernike terms varies slightly. For example, the sensor is two times as sensitive to defocus than totip/tilt aberration.

III. B. Sensor output

Using these Eqs. (2) and (3), a set of sensor signals was generated for a given Zernike term with different magnitudes. The sensor signals of a small but non-zero magnitude A were set as the reference signals for that Zernike term. The sensor output for the given Zernike term of a magnitude was then defined as the best-fit amplitude of the input sensor signals $t_x(i,j)$ and $t_y(i,j)$ referred to the reference signals $\hat{t}_x(i,j)$ and $\hat{t}_y(i,j)$:

$$Sensor\ output = A \frac{\sum_i \sum_j \left(t_x(i,j)\hat{t}_x(i,j) + t_y(i,j)\hat{t}_y(i,j)\right)}{\sum_i \sum_j \left(\hat{t}_x(i,j)\hat{t}_x(i,j) + \hat{t}_y(i,j)\hat{t}_y(i,j)\right)} \tag{5}$$

Fig. 5 shows the sensor output for the first 10 Zernike terms of various magnitudes. This figure shows that, whenthe sensor signal is derived in the way described in this paper, the sensor can linearly measure Zernike terms up to an amplitude of $\pm 0.5 \sim 1.0$ (Noll's definition [12]).

Then the shift δX of the focus due to the tilt could be derived by Fourieroptics [13] to be as:

$$\delta X = \frac{1}{2\pi} \frac{2A}{R} F\lambda \tag{6}$$

where A is the amplitude of the Zernike term in radians and F is the focal length of the system and λ is the operating wavelength.

The simulation shows that the sensor could detect the Z2 of an amplitude A up to a value of$\sim$0.8. In other words, the sensor could detect the tip/tilt component up to a maximumvalue θ_t(in radian) as given by:

$$\theta_t = \frac{\delta X}{F} \approx 0.5 \frac{\lambda}{D} \tag{7}$$

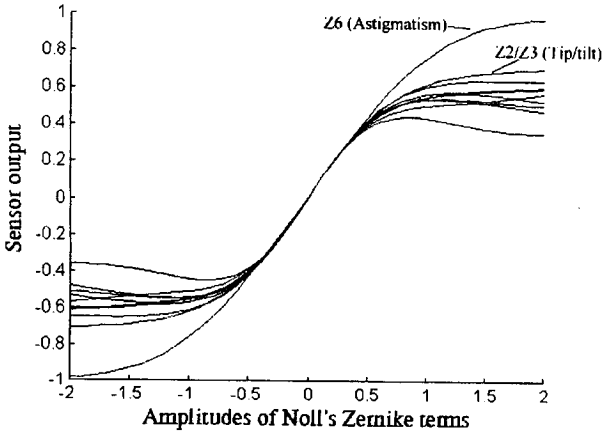

FIG. 5. Sensor output for the first 10 Zernike terms of various amplitudes (unit radian)

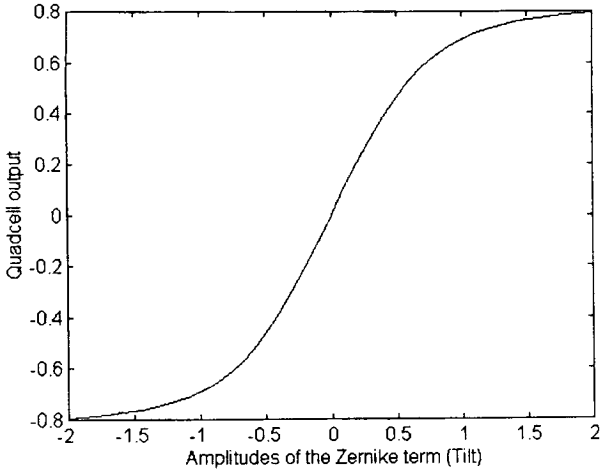

FIG. 6. Quadcell output for the tip/tilt Zernike term (unit radian).

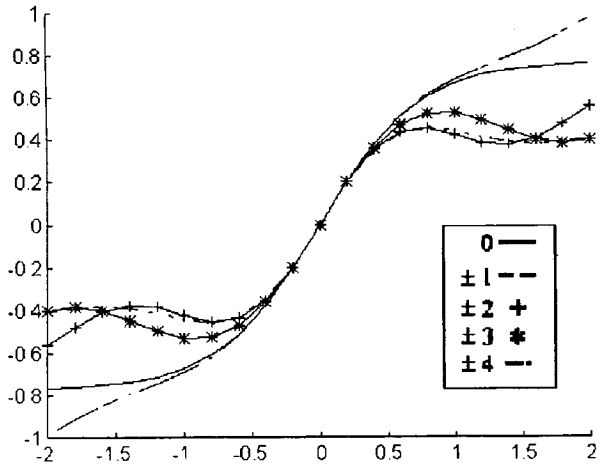

FIG. 7. The sensor output for the tip/tilt aberration (Z2/Z3) considering bevel effects of the prism (unit radian).

where D is the diameter of the aperture.

Eq. (7) shows that maximum detectable tip/tilt angle θ_t is approximately half the maximum angular resolution(1.22λ/D) of a perfect telescope of diameter D. This means that the intensity peakshould be located within half of the Airy radius from the apex of the sensor. This alsorequires that the sensor would be used for only quite well corrected wavefronts in order tohave such a peak. For a system with a diameter of 50 cm, the maximum measurable tilt angle bythis method is about 0.12 arcsec on the sky.

Fig. 6 shows simulated output of a quadcell for tip/tilt wavefront aberrations. Comparison of the result with thepyramidal sensor output (Fig. 5) shows that the pyramidal sensor and a quadcellhave the same linear zone for tip/tilt aberrations. This confirms that the pyramidal sensor is basically a quadcell.

III. C. Effects of the bevel of the sensor apex

The edge (bevel) of optical prisms is sharp but it does have a finite size. Therefore, the rays arriving at the edgeare blocked and scattered by the edge. Since the pupil plane sensor compares the intensities of four pupil images, itshould be investigated how the blocked rays change the four pupil images and therefore the sensor outputs.

To include the effect of finite bevel of the prisms, the simulation was repeated after the image plane (or Fourier plane) of 256×256 pixels was filtered in a way that the central cross pixels (0, ±1, ±2,±3, and ±4 pixels), which represent rays arriving at the finite bevel (edge), were blockedout. Simulation founds out that the sensor becomes more linear to some Zernike terms with afinite edge thickness rather than with a zero thickness. Fig. 7 shows the result ofsimulation for the tip/tilt (Z2/Z3) components. This figure shows that the sensor can be measured best with an edge thickness t of 2 (±1) pixels (among the given five sizes of the edge) in the image plane of256×256 pixels. The thickness t can be shown by Discrete Fourier Transform theory tobe given as

$$t = \lambda(F/\#) \tag{8}$$

For a F/15 telescope, the edge thickness is about 9 μm. The true optimum thickness can be found with finer sampling size.

These results show that the sensor could be manufactured with a finite edge thickness rather than a zero one to improve the linearity of the sensor. The exact thickness should be traded off between the Zernike terms which the sensor is to measure and the manufacturability.

IV. PRELIMINARY EVALUATION

A prototype sensor was manufactured with two crossed biprisms, which ideally are functionally identical to a pyramidal prism.

The first experiment (Fig. 8) was to determine the limiting F/number for the sensor. Four pupil images of the sensorwere recorded as F/number was varied from F/175 to F/14.5 by changing the diameter D of aperture stop. Fig. 9 shows pictures of the four pupil images.

It was shown in Fig. 9 that the measured four pupil images start to overlap from an aperture stop diameter of 16mmindicating that the prototype can be used for systems whose F/numbers are slower than a F/number of F/22.

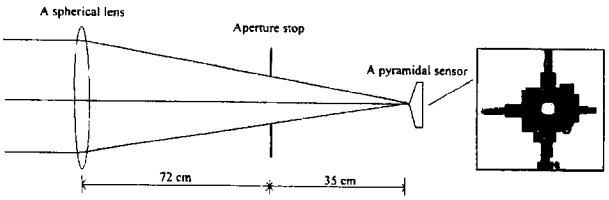

FIG. 8. Schematic optical layout of the experiment with a picture of the sensor

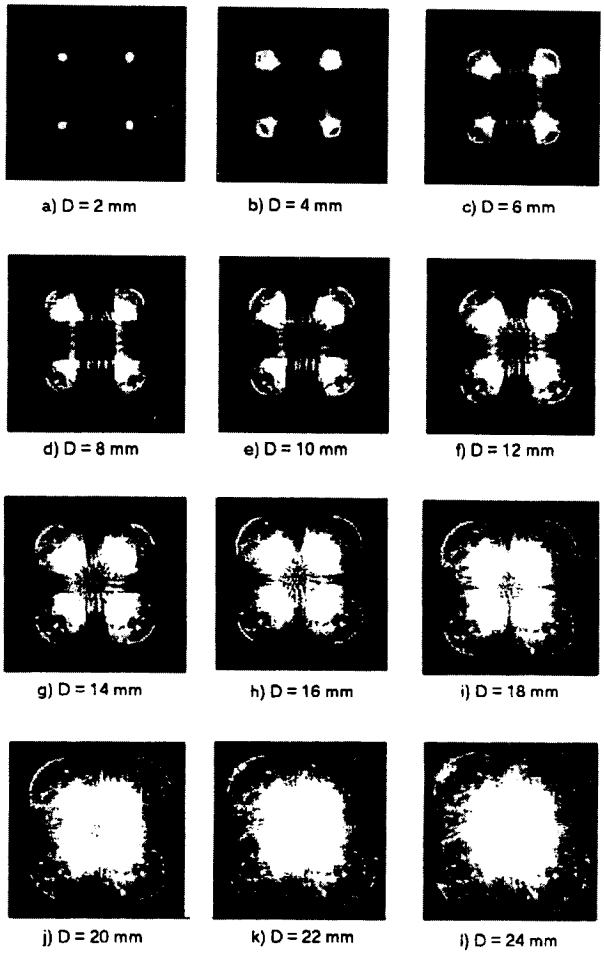

FIG. 9. Measured four pupil images for various aperture sizes from 2 mm (F/175) to 24 mm (F/14.5). D is the size of aperture stop as shown in Fig. 6.

It can be shown by simple geometric optics that a thin pyramidal prism with a slope angleθ_p can split the pupil images without overlapping for the optical systems with aF/number bigger than F_0 given by

$$F_0 \approx \frac{1}{2(n-1)\theta_p} \tag{9}$$

where n is the refractive index of the prism and θ_p is in radians. This equation was confirmedby our prototype prism which has $\theta_p = 2.62\,^\circ$ and $F_0 = 22$.

V. CONCLUSION

This paper presents the four pupil images and the simulated output of the pyramidal sensor for some lower order Zernike terms. The pyramidal sensor is found to provide full wavefront sensing when the intensity peak of PSF is located within half of the Airy radius from the apex of the sensor. This requires that the sensor would be used in this mode for only small wavefront errors.

We have also investigated the effect of finite size of the bevel of the prism apex, concluding that there is an optimumthickness rather than zero thickness for a given task. In addition to this, the prism slope is found to be a function of the maximum F/number (Eq. 9) which the sensor is designed to operate for and a single pyramidal sensor is found tobe preferable to the two crossed biprisms whose finite air gap between the two apex causes defocus.

Further research is required to investigate other characteristics of the sensor such as sensitivity of the sensor under various noise sources. The evaluation will be extended by the help of an adaptive secondary mirror demonstrator being developed at the Optical Science Laboratory(OSL). [14–16]

ACKNOWLEDGMENTS

The work described in this paper has been financed from a number of sources, including the Satellite Technology Center (SaTReC) of the Korea Advanced Institute of Science and Technology (KAIST), the UK Gemini project office, and the UK Particle Physics and Astronomy Research Council.

REFERENCES

[1] J.M. Beckers, Annual Review of Astronomy and Astrophysics **31**, 13 (1993).
[2] C.L. Koliopoulos, Appl. Opt. **19**(9), 1523-1528 (1980).
[3] J.W. Hardy, E.E. Lefebvre, C.L. Koliopoulos, Optical Society of America **67**(3), 360 (1977).
[4] D. Schmutz, E. Lawrence, Proc. SPIE, 13 (1987).
[5] D.V. Murphy, Lincoln Laboratory Journal **5**(1), 25 (1992).
[6] N. Roddier, Appl. Opt. **27**(7), 1223 (1988).
[7] N. Roddier, Proc. SPIE **1542**, 120 (1991).
[8] N. Pugh, D. Lobb, D. Walker, T. Williams, Proc. SPIE, **2534**, 312 (1995).
[9] R. Ragazzoni, Journal of modern optics **43**(2), 289 (1996).
[10] *MATLAB*, The MathWorks, Inc., 24 Prime Park Way, Natick, Mass., USA

[11] E. O. Brigham, *The Fast Fourier Transform*, (Prentice-Hall, New York, 1974).
[12] R. J. Noll, J. Opt. Soc. Am. **A 66**(3), 207 (1976).
[13] G. O. Reynolds, J. B. DeVelis, G. B. Parrent Jr, B. J. Thompson, *The new Physical Optics Notebook: Tutorials in Fourier Optics*, SPIE Optical Engineering Press, 1989.
[14] J. H. Lee, D. D. Walker, A. P. Doel, Opt. Eng. **38**, 1456 (1999).
[15] J. H. Lee, B. B. Bigelow, D. D. Walker, A.P.Doel, R.G.Bingham, "Why Adaptive Secondaries?", Publications of the Astronomical Society of the Pacific (PASP), Jan., 112:97-107, 2000.
[16] J. H. Lee, D. D. Walker, A. P. Doel, Optical Engineering, April (2000), in press.